TU Delft

Delft University of Technology

Armor Damage On Groins Under Ship Wave Attack Using Field Data

Mares Nasarre, Patricia; Morales Napoles, Oswaldo; Hofland, Bas; Melling, Gregor

DOI
10.59490/coastlab.2024.706

Publication date
2024

Document Version
Final published version

Citation (APA)
Mares Nasarre, P., Morales Napoles, O., Hofland, B., & Melling, G. (2024). *Armor Damage On Groins Under Ship Wave Attack Using Field Data*. Paper presented at 9th Conference on Physical Modelling in Coastal Engineering and Science, CoastLab 2024, Delft, Netherlands. https://doi.org/10.59490/coastlab.2024.706

Important note
To cite this publication, please use the final published version (if applicable).
Please check the document version above.

Copyright
Other than for strictly personal use, it is not permitted to download, forward or distribute the text or part of it, without the consent of the author(s) and/or copyright holder(s), unless the work is under an open content license such as Creative Commons.

Takedown policy
Please contact us and provide details if you believe this document breaches copyrights.
We will remove access to the work immediately and investigate your claim.

This work is downloaded from Delft University of Technology.
For technical reasons the number of authors shown on this cover page is limited to a maximum of 10.

Proceedings of the 9th International Conference on Physical Modelling in Coastal Engineering (Coastlab24)
Delft, Netherlands, May 13-16, 2024
©2024 published by TU Delft OPEN Publishing on behalf of the authors
This work is licensed under a CC BY 4.0
Conference Paper, DOI: 10.59490/coastlab.2024.706

ARMOR DAMAGE ON GROYNES UNDER SHIP WAVE ATTACK USING FIELD DATA

PATRICIA MARES-NASARRE[1], OSWALDO MORALES-NÁPOLES[1], BAS HOFLAND[1], GREGOR MELLING[2],

1 Delft University of Technology, the Netherlands, p.maresnasarre@tudelft.nl, o.moralesnapoles@tudelft.nl, b.hofland@tudelft.nl,
2 Federal Waterways Engineering and Research Institute (BAW), Germany, gregor.melling@baw.de

ABSTRACT

The severity of damages to riverine structures, such as groynes or revetments, across German estuaries has increased in the past years due to the increase in the ship-induced loads. However, few studies can be found in the literature focused on the damage of rock slopes under ship wave attack. In this study, the field data of a rock-armored groyne (lateral slope 1/4 and rocks with nominal diameter D_{n50}≈12.6cm and high density ρ_s=3.7t/m^3) tracked for a year by Melling et al. (2020) is analyzed; the field campaign began after the structure was rebuilt and finished when the structure already presented severe damage. During this field campaign, the incident ship-induced primary waves and water levels were recorded, and laser scans of the groyne armor were taken. Using those field laser scans, damage curves along the life of the structure were derived. Also, ship data from the AIS was retrieved. Then, each increment of the damage (increment of the dimensionless eroded area, ΔS_e) was related to a ship-wave event and a passing ship. The most significant variable to describe ΔS_e was found to be the primary wave height H_p, while the best explanatory variables for H_p were the partial blockage factor, the ship length and width and the relative velocity of the ship. The shape of the dependence between these variables is also analyzed by pairs using copula space. A clear tail dependence is observed between several pairs. For instance, the pair ΔS_e and H_p presents upper tail dependence, meaning that the high values of ΔS_e and H_p are more correlated than the smaller ones. This implies that models more complex than Gaussian copula, which is commonly used in Coastal Engineering applications, might be needed to model the probabilistic dependence between the variables.

KEYWORDS: Armor Damage, Ship Waves, Field Measurements, Probabilistic Dependence, Rock Groyne, Wave-Structure Interaction, Rock Armor

1 INTRODUCTION

An increase in the severity of damages to riverine structures, such as groynes or revetments, was observed across German estuaries in the past years. Investigations into the causes point out to the increase in the ship-induced loads due to the changes in the shipping fleet, such as the ever-increasing dimensions of the container vessels (BAW, 2010). However, little literature is available on the damage of rock slopes under ship wave attack.

Physical model tests on the hydraulic stability of the armor layer of rubble mound breakwaters under sea wave attack are common practice in scientific literature (e.g.: Mares-Nasarre et al., 2021, 2022). However, physical experiments on groyne stability attacked by long-period ship waves are relatively novel and, thus, data from laboratory is scarce and limited. In this study, the damage of a rock-armored groyne under ship-wave attack is studied using damage measurements from a field campaign described in Melling et al. (2020). First, the field laser scans are processed to obtain damage curves during the monitoring period of one year. Later, the relationship between the damage and various loading variables (e.g.: primary wave height, H_p, or ship width, W_S) is explored from a probabilistic point of view using Spearman's rank correlations (Spearman, 1904) and bivariate copulas. This analysis aims to bring light into the relationship between the ship characteristics, the loading conditions, and the generated damage.

2 FIELD DATA

Melling et al. (2020) rebuilt two groynes in the tidal Lower Elbe with two innovative designs (one with a large-radius root, G1, and one with a recessed root, G2) with a view to increase structure stability. Both structures were rock-armored with a gentle lateral slope (1/4) and were tracked for a year. Here, groyne G1 is further investigated; G1 was covered with a rock grading CP90/250 (median rock size D_{50}=15cm, so D_{n50}≈0.84×15=12.6cm according to CIRIA/CUR/CETMEF, 2007) with iron-silicate rocks of high density (ρ_s=3.7t/m^3). Groyne G1 reached the qualitative damage level of Destruction at the end of

tracking period (Losada et al., 1986; Vidal et al., 1991). The incident ship-induced waves and water levels were recorded using pressure sensor gauges; here the measurements of the pressure gauge located at the upstream toe of a trunk section of the groyne are used (see Figure 1(a)). Ship data from the Automatic Identification System database (AIS) was also retrieved to identify which ship provoked each ship-wave event. The armour layer deformation was recorded using a terrestrial, pile mounted laser (see Figure 1(a)). These field laser scans had a resolution of 25cm.

2.1. Measuring quantitative damage

Based on the uncertainty analysis in BAW (n.d.), the closer to the root, where the laser was deployed, the lower the uncertainty in the measurements. Thus, the cross-sections to study are chosen in the proximity of the root. In order to select them, the difference in the measured elevations between the reference scan (10th July 2015) and the last scan (maximum measured damage) are plotted and the biggest defect close to the root is selected to characterize the damage of the structure. Three cross sections are selected with a spacing of 1 meter between them to characterize such defect, as depicted in Figure 1(a). These three cross sections were selected to characterize damage since they belong to one of the largest defects of the structure while being within the most reliable sections in the scans. Also, the selection and cleaning of the scans was time consuming and location-dependent, making unfeasible to average the scans along an entire width. The qualitative damage of the armor layer is described by a single defect being large enough to allow the filter layers to be washed away (Losada et al., 1986; Vidal et al., 1991). Thus, a single defect can hinder the whole structure integrity and the damage per defect needs to be taken into account.

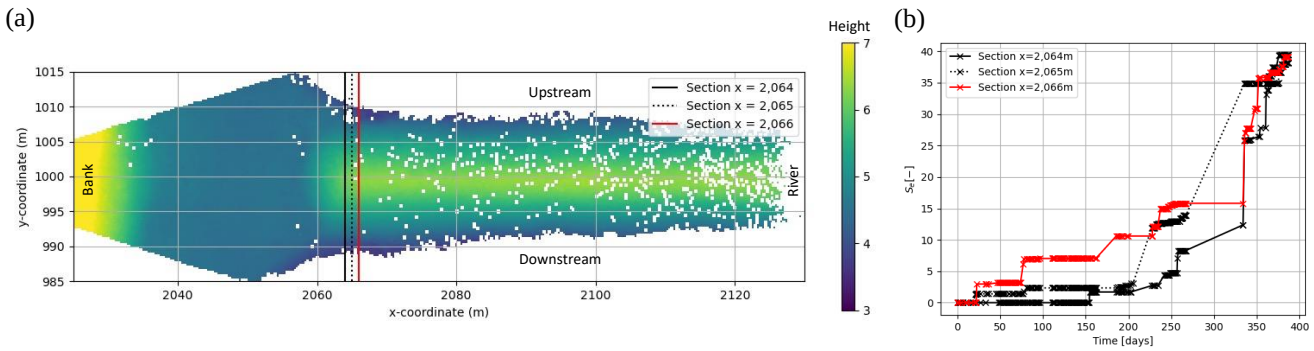

Figure 1. Field damage data: (a) example of a laser scan, and (b) derived damage curves in three cross-sections.

In this study, the laser scans used to record the armor layer deformation of G1 are processed to derive damage curves during the monitoring period of the structure (see Figure 1(b)). The dimensionless armor damage parameter, S_e, defined in Broderick (1983) is used to quantify armor damage as

$$S_e = \frac{A_e}{{D_{n50}}^2} \quad (1)$$

where A_e is the width-averaged eroded cross-sectional area. This area is calculated by comparing the cross-section in the reference scan with the same cross-section in the subsequent scans; the eroded area is integrated. Note that here each cross-section is treated independently, so the eroded area is not averaged as in Broderick (1983). The following operations were performed in order to allow this computation: (1) alignment of the cross-sections (displacement of the section in the vertical direction) using the highest point of the cross-section (no erosion point), (2) linear interpolation between the observations to obtain the same grid and allow the comparison between cross-sections, and (3) only those points where the differences with the cross-section from the reference scan were higher than 5cm after the alignment were considered in the eroded area.

Once A_e is computed for each laser scan, S_e is calculated and accumulated over time to obtain the cumulative damage curves. Note that not all the scans could be used in the process due to inaccuracies or disruptions in the deployment (e.g.: a seagull on top of the structure). Figure 1(b) presents the damage curves of the cross sections in Figure 1(a).

Individual damage events are identified along the obtained cumulative damage curves (ΔS_e) and related to the loading conditions to analyze their probabilistic dependence. Each increase in the damage curve was assumed to be attributed to one ship-wave event. Thus, ΔS_e was associated with a concomitant ship passage and ship-induced wave as the largest event in terms of H_p which happened between that scan and the previous one. For each cross-section, between 15 and 22 events were identified.

To determine whether the pre-existing S_e conditionalizes the next ΔS_e caused by a ship-wave event (memory of the process), the Spearman's correlation coefficient (R) is calculated between the S_e at time step t and ΔS_e at time step $t+1$. -0.20 $\leq R \leq$ 0.40 were obtained with *p-values*>0.05, meaning that the observed correlations are not significant. Therefore, ΔS_e for

each event can be analyzed independently.

3 RESULTS

The relationship between the individual damage measurements, the ship-induced waves and the ship passages is analyzed here. The following variables are considered: the increment of the damage (ΔS_e), the primary wave height (H_p), the stern wave period (T_{ST}), the ambient water level (h), the ship length (L_s), the ship width (W_s), the relative velocity of the ship ($V_{s,rel}$), the ship draft (D_s) and the partial blockage factor ($nT=A_{cp}/A_{sp}$, where A_{sp} is half of the cross sectional area of the submerged part of the ship and A_{cp} is the cross sectional area of the waterway from the edge of the ship to the margin of the waterway). In Figure 2, the definition of these variables is presented.

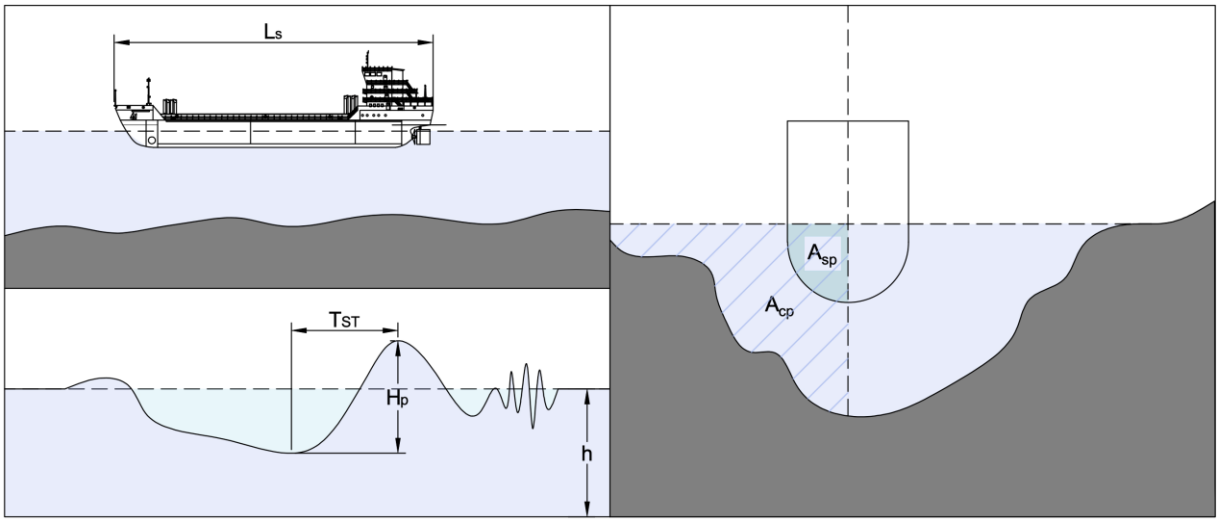

Figure 2. Ship-wave variables definition.

3.1. Rank correlations

Here, the rank correlation matrix is computed to see the strength of the dependence between each pair of variables. Also, the associated *p-values* are computed to assess the significance of the observed correlations. Note that here *p-values* represent the probability of the observed correlation not being significant. Thus, *p-values*<0.05 indicate a significant correlation.

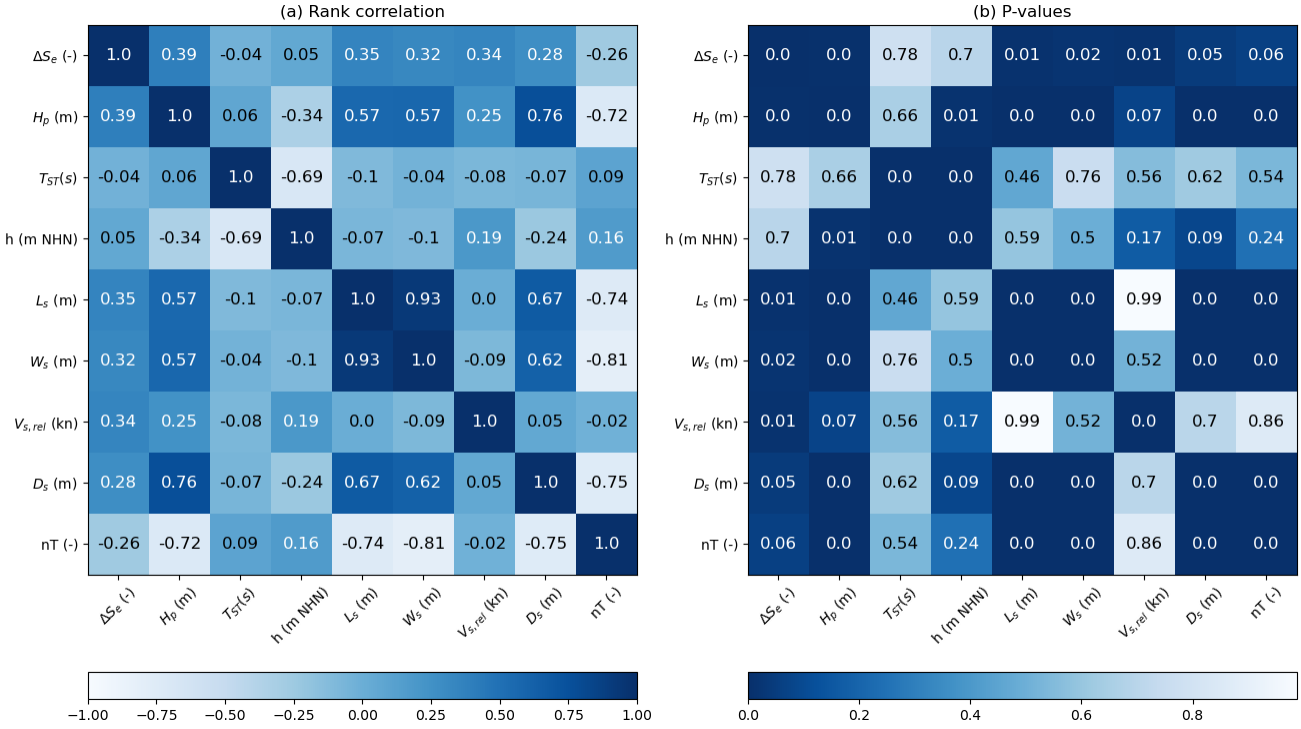

Figure 3. Correlation matrix between each pair of variables: (a) rank correlations, and (b) associated p-values.

Focusing on ΔS_e, the highest correlations are those with H_p, L_s, W_s and $V_{s,rel}$ with $0.32 \leq R \leq 0.39$, being all of them also significant. The main driver of damage is the ship-wave attack, so a significant rank correlation between ΔS_e and H_p is expected. L_s and W_s are strongly related to each other due to the ship's shape and present also a high significant rank correlation R=0.59 with H_p. Thus, it is inferred that the dimensions of the ship (L_s and W_s) influence the generated ship-induced wave and, by that, the damage in the groyne. $V_{s,rel}$ only presents a significant rank correlation with ΔS_e, although that with H_p is close to the selected significance level. Thus, we can conclude that the main variable within those analyzed in this study to describe ΔS_e is H_p.

Moving now to H_p, the highest correlations in absolute value are those with D_s and nT with R=0.76 and -0.72, respectively, and significant *p-values*. Note that D_s is included to nT and, thus, a high negative correlation between the variables can also be observed (R=-0.75). The next highest rank correlations are those with L_s and W_s, as previously discussed, h and $V_{s,rel}$. Thus, the main explanatory variables for H_p would be L_s, W_s, $V_{s,rel}$ and nT, which includes D_s and h.

3.2. Shape of the dependence

In this section, the shape of the dependence between the bivariate pairs identified as relevant in the previous section is inspected. In order to analyze the dependence between the variables without the influence of the marginals, copula space or unity space is used here. According to Sklar (1959), any multivariate joint distribution of continuous variables can be described as a set of univariate marginal distributions and a copula that models the dependence between the variables. The definition of copula for the bivariate case is given by

$$H_{X1,X2}(x_1, x_2) = C(F_{X1}(x_1), F_{X2}(x_2)) \tag{2}$$

where $H_{X1,X2}(x_1, x_2)$ for $(x_1, x_2) \in \mathbb{R}^2$ is a joint distribution with marginals $F_{X1}(x_1)$ and $F_{X2}(x_2)$ in [0, 1] and a copula in the unit square $I^2 = ([0,1] \times [0,1])$, being Eq. (2) satisfied for all $(x_1, x_2) \in \mathbb{R}^2$.

The observations are then transformed to unity space and, afterwards, for better visualization, the observations in unity space are transformed to standard normal space, as shown in Figure 3.

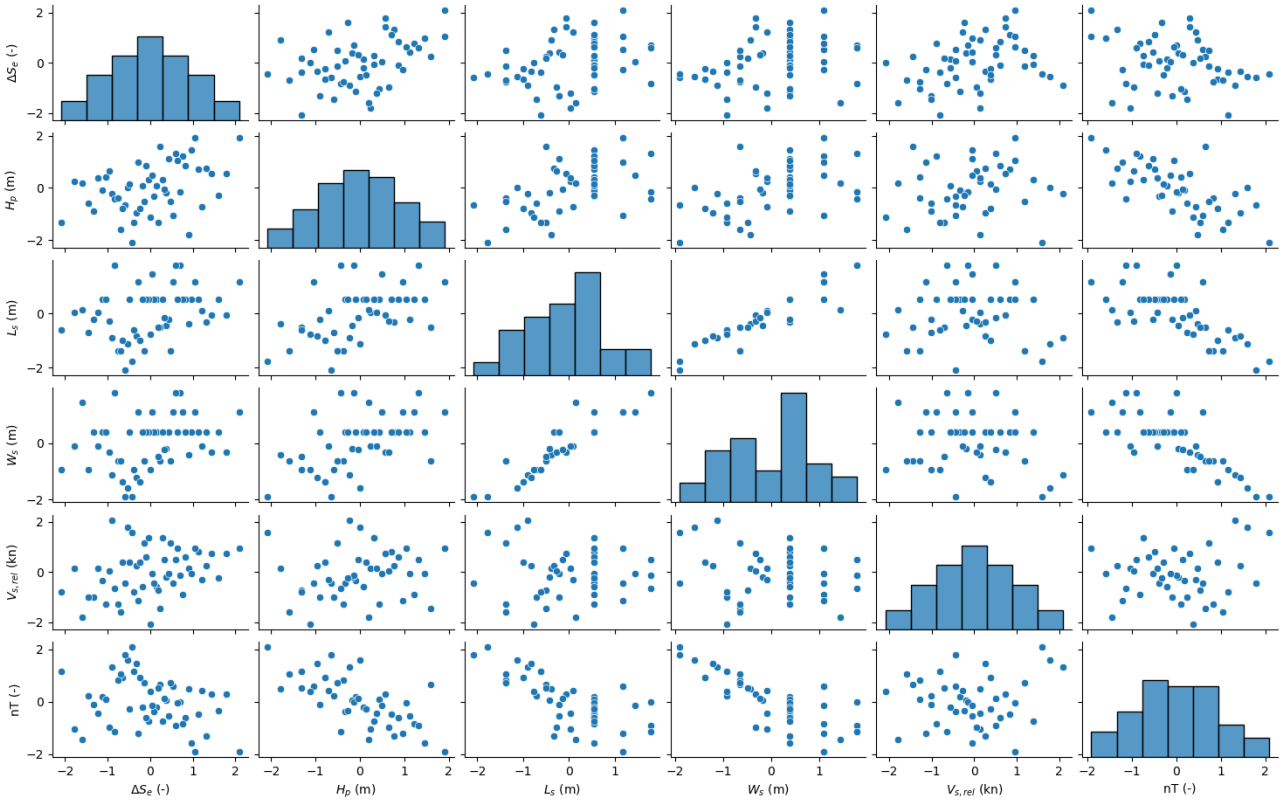

Figure 4. Scatter matrix of the observations in standard normal space.

As shown in the top second left panel in Figure 4, there is a positive tail dependence in the pair ΔS_e and H_p. This is, the high values of ΔS_e and H_p are more correlated than the smaller ones. Lower tail dependence (higher correlation between lower values of the random variables) is observed in the pairs H_p and L_s, H_p and W_s, L_s and nT, W_s and nT, and L_s and W_s. Therefore,

the simplest copula model, Gaussian copula, which is commonly used in the Coastal Engineering field (e.g.: Camus et al., 2019; Lucio et al., 2020) might not be suitable to model the dependence between these pairs.

4 CONCLUSIONS

The increase in the ship-induced loads caused by the changes in the shipping fleet has increased the severity of damages to riverine structures, such as groynes or revetments, across German estuaries in the past years. However, little literature is available on the damage of rock slopes under ship wave attack.

In this study, the field laser scans of a rock-armored groyne that Melling et al. (2020) tracked for a year are analyzed. Note that the field campaign started after the reconstruction of the structure and finished when the structure had already reached severe damage. The rock-armored groyne presented a gentle lateral slope (1/4), a rock grading CP90/250 (D_{n50}≈12.6cm) with iron-silicate rocks of high density (ρ_s=3.7t/m^3). Using those field laser scans, damage curves along the life of the structure were derived. The incident ship-induced waves and water levels were also recorded and ship data from the AIS was retrieved. Then, each increment of damage (ΔS_e) could be linked to a ship-wave event as the maximum between the time of that scan and the time of the previous scan.

The most significant variables to describe ΔS_e and H_p are selected based on the rank correlations and their associated p-values. The following variables are considered: ΔS_e, the primary wave height (H_p), the stern wave period (T_{ST}), the ambient water level (h), the ship length (L_s), the ship width (W_s), the relative velocity of the ship ($V_{s,rel}$), the ship draft (D_s) and the partial blockage factor ($nT=A_{sp}/A_{cp}$, see Figure 2). The best variable within those analyzed in this study to describe ΔS_e was found to be H_p, while the main explanatory variables for H_p would be nT, L_s, W_s and $V_{s,rel}$.

The shape of the dependence between ΔS_e, H_p and the variables previously identified as the most relevant ones to described them (nT, L_s, W_s and $V_{s,rel}$) is also analyzed for each pair using copula space. A clear tail dependence is observed between several pairs. For instance, the pair ΔS_e and H_p presents upper tail dependence so the high values of ΔS_e and H_p are more correlated than the smaller ones. This might imply that models more complex than Gaussian copula, which is commonly used in Coastal Engineering applications, might be needed to model the probabilistic dependence between these variables.

ACKNOWLEDGEMENT

This research was funded by the Federal Waterways Engineering and Research Institute (BAW) as part of the research project “ProbBem”.

REFERENCES

BAW. (n.d.). *Scan grid - raster uncertainty - c2c z distance*.

BAW. (2010). *Bemessung der Strombauwerke in der Außenweser unter Berücksichtigung von Schiffswellenbelastungen (BAW-Gutachten, A39550210120)*.

Broderick, L. L. (1983). Riprap stability a progress report. *Proc. Specialty Conference on Design, Construction, Maintenance and Performance of Coastal Structures*, 320–330.

Camus, P., Tomás, A., Díaz-Hernández, G., Rodríguez, B., Izaguirre, C., & Losada, I. J. (2019). Probabilistic assessment of port operation downtimes under climate change. *Coastal Engineering*, *147*, 12–24. https://doi.org/10.1016/j.coastaleng.2019.01.007

CIRIA/CUR/CETMEF. (2007). *The Rock Manual. The use of rock in hydraulic engineering* (CIRIA, Ed.; Second edition).

Losada, M. A., Desire, J. M., & Alejo, L. M. (1986). Stability of Blocks as Breakwater Armor Units. *Journal of Structural Engineering*, *112*(11), 2392–2401. https://doi.org/10.1061/(ASCE)0733-9445(1986)112:11(2392)

Lucio, D., Tomás, A., Lara, J. L., Camus, P., & Losada, I. J. (2020). Stochastic modeling of long-term wave climate based on weather patterns for coastal structures applications. *Coastal Engineering*, *161*, 103771. https://doi.org/10.1016/j.coastaleng.2020.103771

Mares-Nasarre, P., Argente, G., Gómez-Martín, M. E., & Medina, J. R. (2021). Armor Damage of Overtopped Mound Breakwaters in Depth-Limited Breaking Wave Conditions. *Journal of Marine Science and Engineering*, *9*(9), 952. https://doi.org/10.3390/jmse9090952

Mares-Nasarre, P., Molines, J., Gómez-Martín, M. E., & Medina, J. R. (2022). Hydraulic stability of cube-armored mound breakwaters in depth-limited breaking wave conditions. *Ocean Engineering*, *259*, 111845. https://doi.org/10.1016/j.oceaneng.2022.111845

Melling, G., Jansch, H., Kondziella, B., Uliczka, K., & Gätje, B. (2020). Evaluation of optimised groyne designs in response to long-period ship wave loads at Juelssand in the Lower Elbe Estuary. *Die Küste 89. Karlsruhe: Bundesanstalt Für Wasserbau*, 29–56. https://doi.org/https://doi.org/10.18171/1.089103

Sklar, M. (1959). Fonctions de repartition a n dimensions et leurs marges. *Publ. Inst. Statist. Univ. Paris*, *8*, 229–231.

Spearman, C. (1904). The proof and measurement of association between two things. *The American Journal of Psychology*, *15*(1), 72–101.

Vidal, C., Losada, M. A., & Medina, R. (1991). Stability of Mound Breakwater's Head and Trunk. *Journal of Waterway, Port, Coastal, and Ocean Engineering*, *117*(6), 570–587. https://doi.org/10.1061/(ASCE)0733-950X(1991)117:6(570)